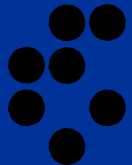


Electron Screening in Nickel

Matej Lipoglavšek

Jožef Stefan Institute, Ljubljana, Slovenia



Split, September 2011

Electron Screening

Due to Coulomb repulsion the cross section σ for charged particle induced nuclear reactions drops rapidly with decreasing beam energy.

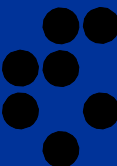
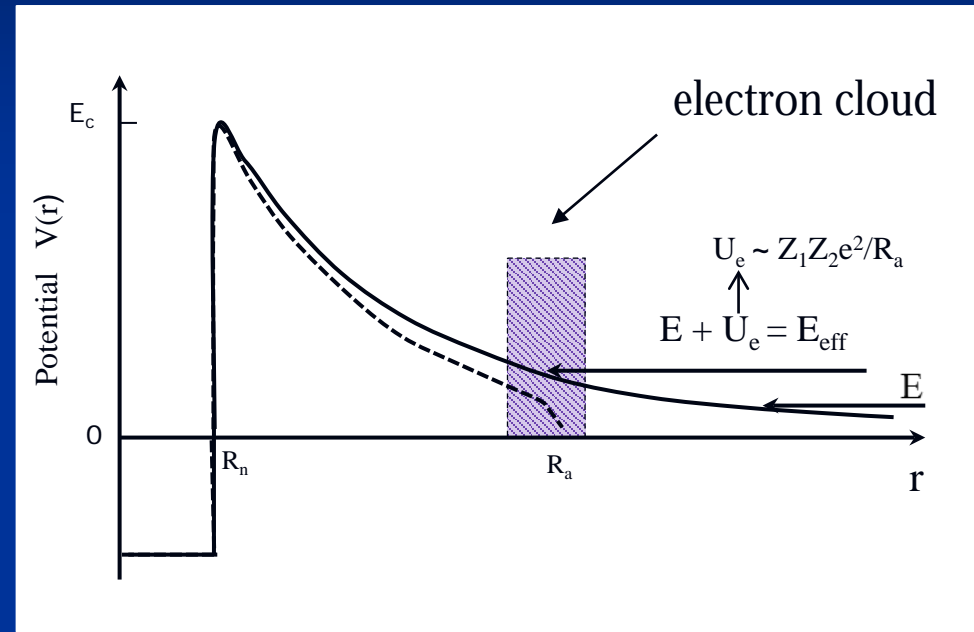
$$s(E) = \frac{S(E)}{E} e^{-2\eta},$$

where $\eta = Z_1 Z_2 e^2 / 4\pi\epsilon_0 \hbar v$ is the Sommerfeld parameter.

Cross section increases at low energies when the interacting nuclei are not bare.

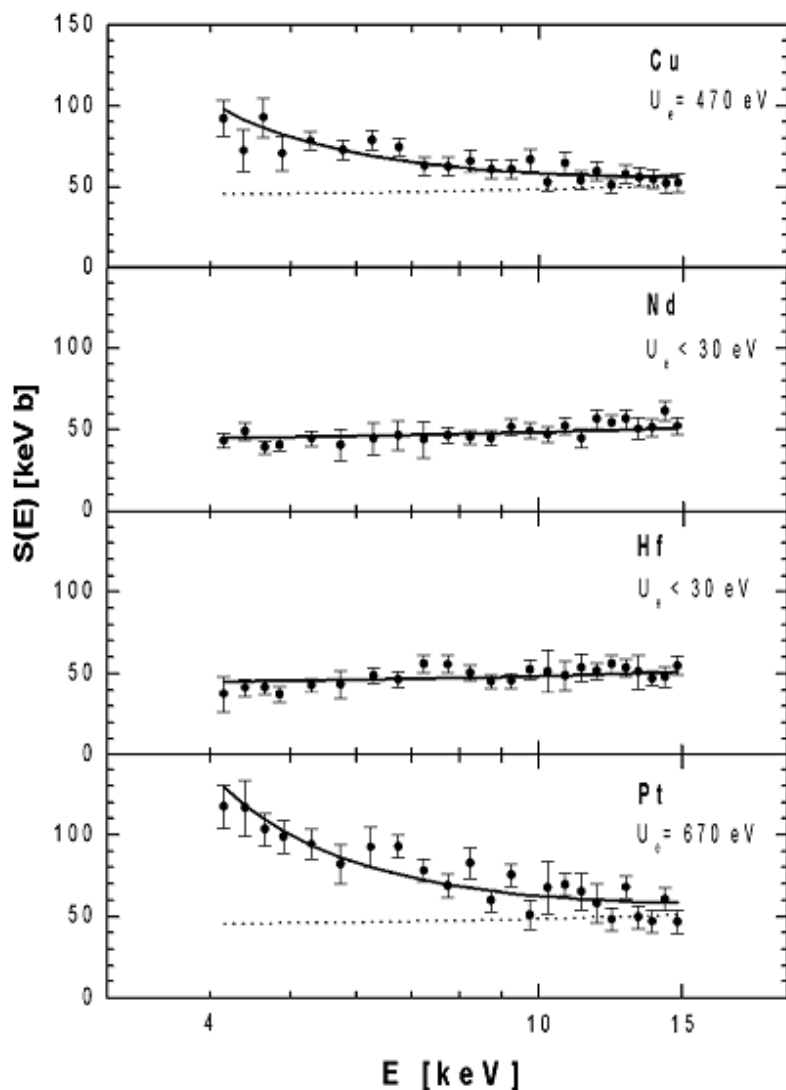
$$f(E) = \frac{s(E + U_e)}{s(E)},$$

where U_e is the screening potential.



Previous Results 1

for $d(d,p)t$ reaction from F. Raiola et al., Eur. Phys. J. A19 (2004) 283.



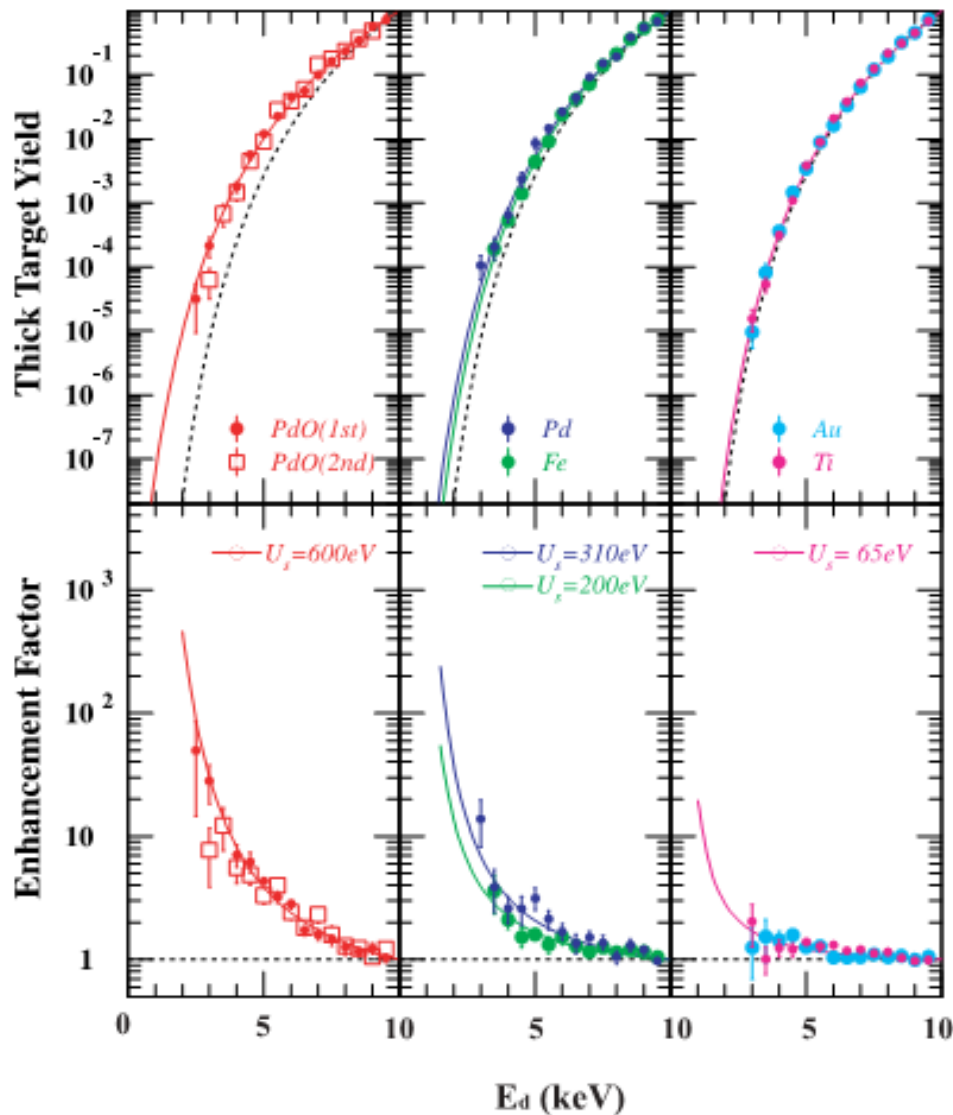
| Material | U_e (eV) ^(b) | Solubility $1/x$ ^(c) | n_{eff} ^(b) | n_{eff} (Hall) ^(d) |
|----------|------------------------------|------------------------------------|---------------------------------|--|
| Metals | | | | |
| Be | 180±40 | 0.08 | 0.2±0.1 | (0.21±0.04) |
| Mg | 440±40 | 0.11 | 3.0±0.5 | 1.8±0.4 |
| Al | 520±50 | 0.26 | 3.0±0.6 | 3.1±0.6 |
| V | 480±60 | 0.04 | 2.1±0.5 | (1.1±0.2) |
| Cr | 320±70 | 0.15 | 0.8±0.4 | (0.20±0.04) |
| Mn | 390±50 | 0.12 | 1.2±0.3 | (0.8±0.2) |
| Fe | 460±60 | 0.06 | 1.7±0.4 | (3.0±0.6) |
| Co | 640±70 | 0.14 | 3.1±0.7 | (1.7±0.3) |
| Ni | 380±40 | 0.13 | 1.1±0.2 | 1.1±0.2 |
| Cu | 470±50 | 0.09 | 1.8±0.4 | 1.5±0.3 |
| Zn | 480±50 | 0.13 | 2.4±0.5 | (1.5±0.3) |
| Sr | 210±30 | 0.27 | 1.7±0.5 | |
| Nb | 470±60 | 0.13 | 2.7±0.7 | (1.3±0.3) |
| Mo | 420±50 | 0.12 | 1.9±0.5 | (0.8±0.2) |
| Ru | 215±30 | 0.18 | 0.4±0.1 | (0.4±0.1) |
| Rh | 230±40 | 0.09 | 0.5±0.2 | (1.7±0.4) |
| Pd | 800±90 | 0.03 | 6.3±1.3 | 1.1±0.2 |
| Ag | 330±40 | 0.14 | 1.3±0.3 | 1.2±0.3 |
| Cd | 360±40 | 0.18 | 1.9±0.4 | (2.5±0.5) |
| In | 520±50 | 0.02 | 4.8±0.9 | |
| Sn | 130±20 | 0.08 | 0.3±0.1 | |
| Sb | 720±70 | 0.13 | 11±2 | |
| Ba | 490±70 | 0.21 | 9.9±2.9 | |
| Ta | 270±30 | 0.13 | 0.9±0.2 | (1.1±0.2) |
| W | 250±30 | 0.29 | 0.7±0.2 | (0.8±0.2) |
| Re | 230±30 | 0.14 | 0.5±0.1 | (0.3±0.1) |
| Ir | 200±40 | 0.23 | 0.4±0.2 | (2.2±0.5) |
| Pt | 670±50 | 0.06 | 4.6±0.7 | 3.9±0.8 |
| Au | 280±50 | 0.18 | 0.9±0.3 | 1.5±0.3 |
| Tl | 550±90 | 0.01 | 5.8±1.2 | (7.4±1.5) |
| Pb | 480±50 | 0.04 | 4.3±0.9 | |
| Bi | 540±60 | 0.12 | 6.9±1.5 | |

Previous Results 2

J. Kasagi, Prog. Theo. Phys. Suppl. 154 (2004) 365

for the $d(d,p)t$ reaction
 $U_e = 310 \pm 30$ eV @ 7% H/Pd

=> concentration dependence



Previous Results 3

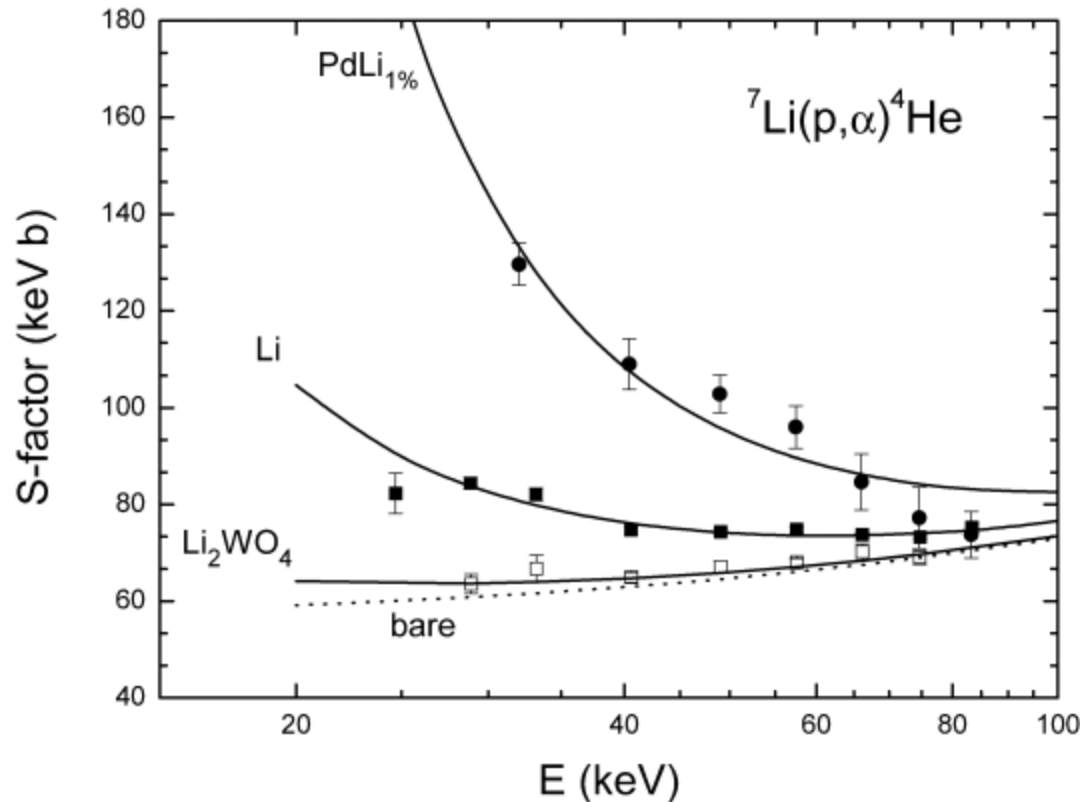
J. Cruz et al., Phys. Lett. B 624 (2005) 181.

For PdLi_{1%}:

$$S(E) = 0.055 + 0.21E - 0.31E^2$$

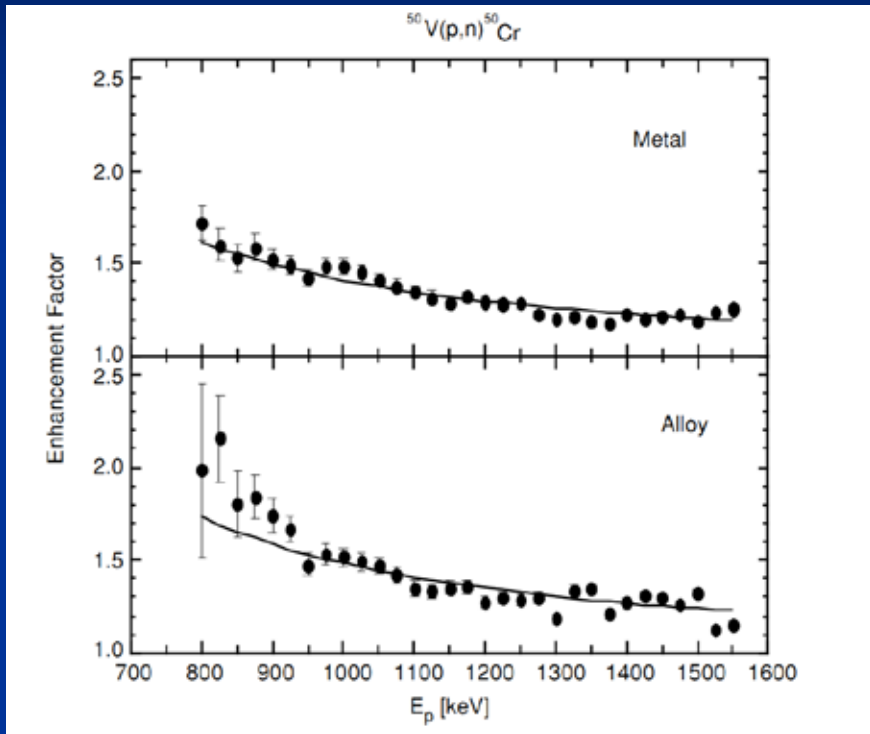
[MeV b]

$$U_e = 3.8 \text{ keV}$$

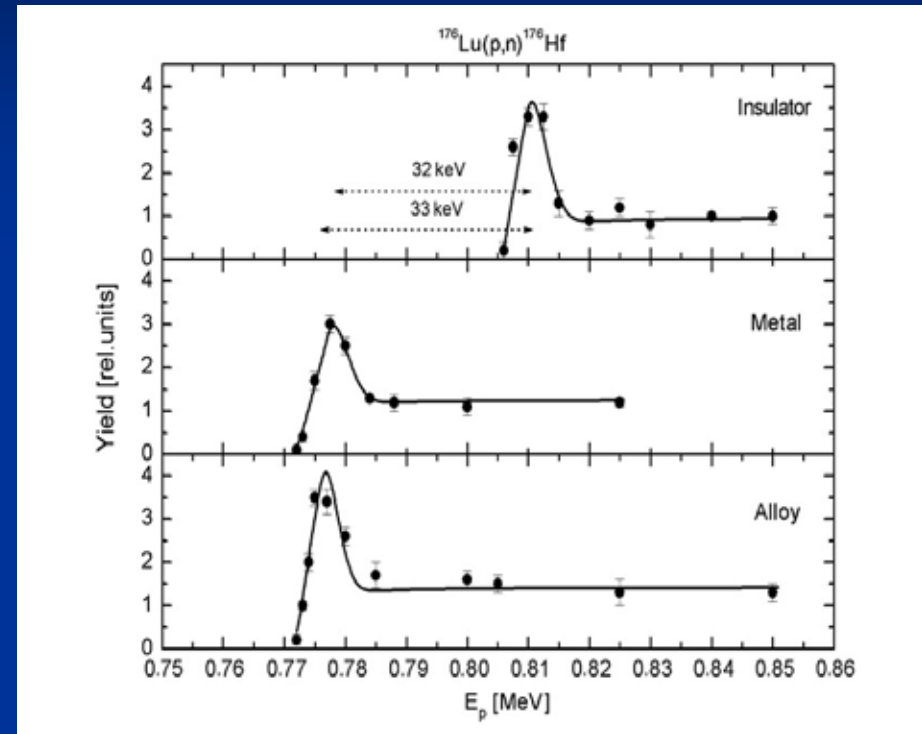


Previous Results 4

K. U. Kettner et al., J. Phys. G **32** (2006) 489.



$^{50}\text{V}(p,n)^{50}\text{Cr}$ reaction in different environments: VO_2 **insulator**, V metal and $\text{PdV}_{10\%}$ alloy. Relative to the insulator, metal and alloy showed a large screening potential of $U_e = 27$ and **34 keV**.



$^{176}\text{Lu}(p,n)^{176}\text{Hf}$ reaction in Lu_2O_3 **insulator**, Lu metal and $\text{PdLu}_{10\%}$ alloy; there is a narrow resonance and a shift in proton resonance energy of $U_e = 32$ and **33 keV** for the metal and alloy, respectively, relative to the **insulator**.

$$\Rightarrow U_e \propto Z$$

Measurements @ JSI



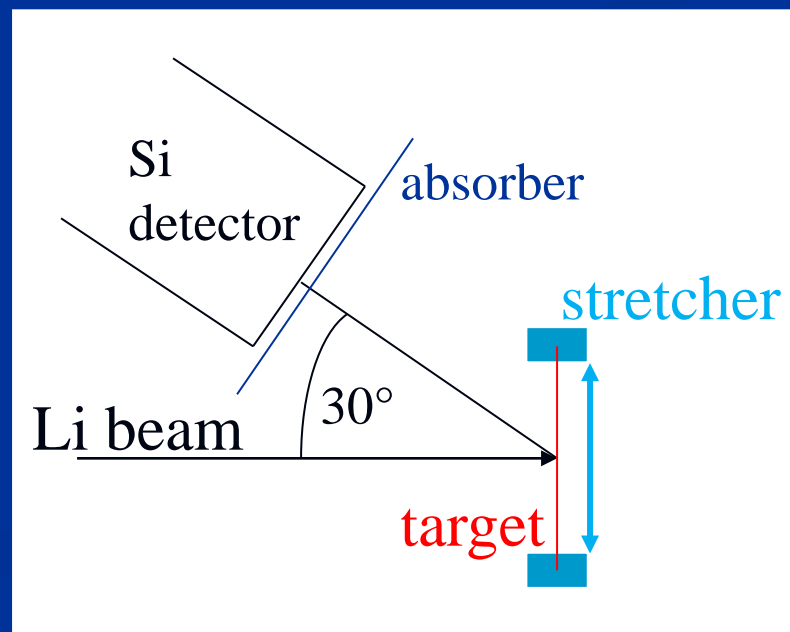
2 MV Tandem van de Graaf accelerator

Reaction: ${}^1\text{H}({}^7\text{Li},\alpha){}^4\text{He}$

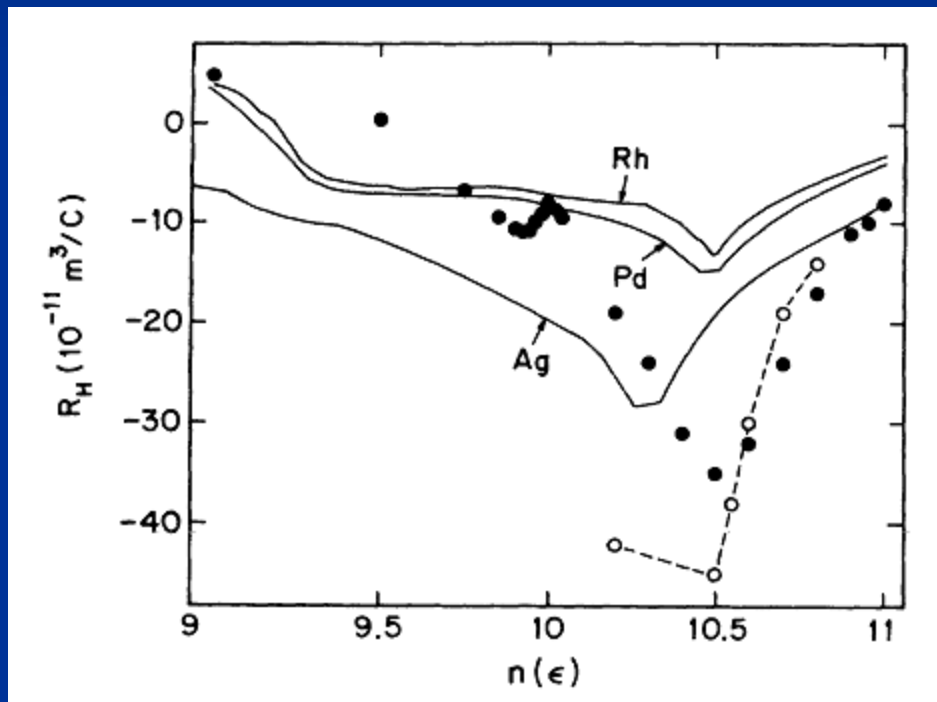
targets:

Kapton (insulator),

Pd, Pd₇₇Ag₂₃ (metals)



Hall Coefficient in PdAg Alloys



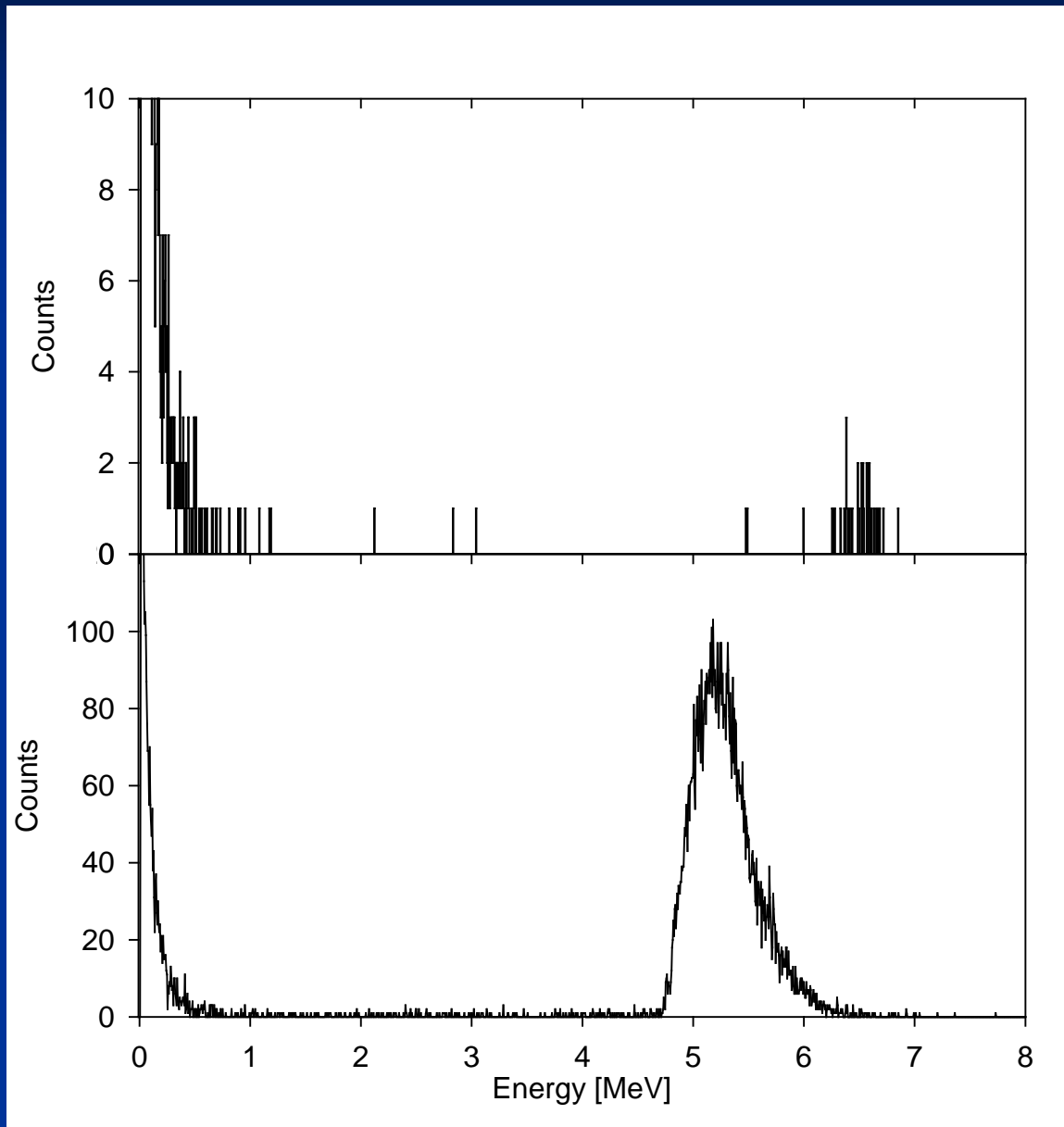
$$R_H(\text{Pd}) = -7 \cdot 10^{-11} \text{ m}^3/\text{As}$$

$$R_H(\text{Pd}_{50}\text{Ag}_{50}) = -35 \cdot 10^{-11} \text{ m}^3/\text{As}$$

$$|R_H| \mu = \frac{1}{n_{eff}}$$

Phys. Rev. B 45 (1992) 10886.

α -particle spectra

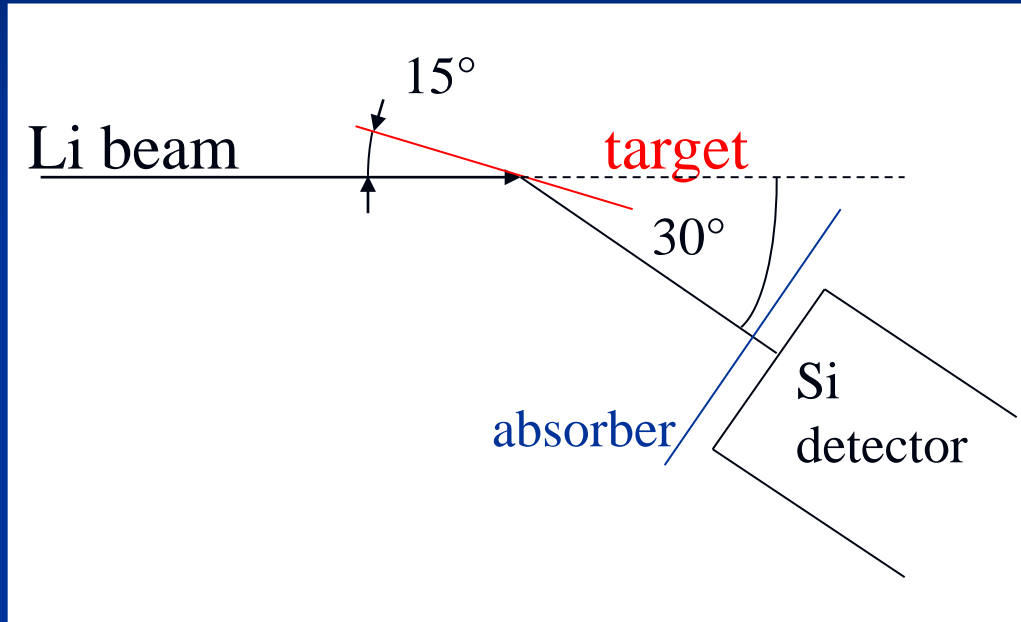


on Kapton @ 340 keV
Li beam energy

on Pd with 43% H
@ 1.05 MeV
Li beam energy

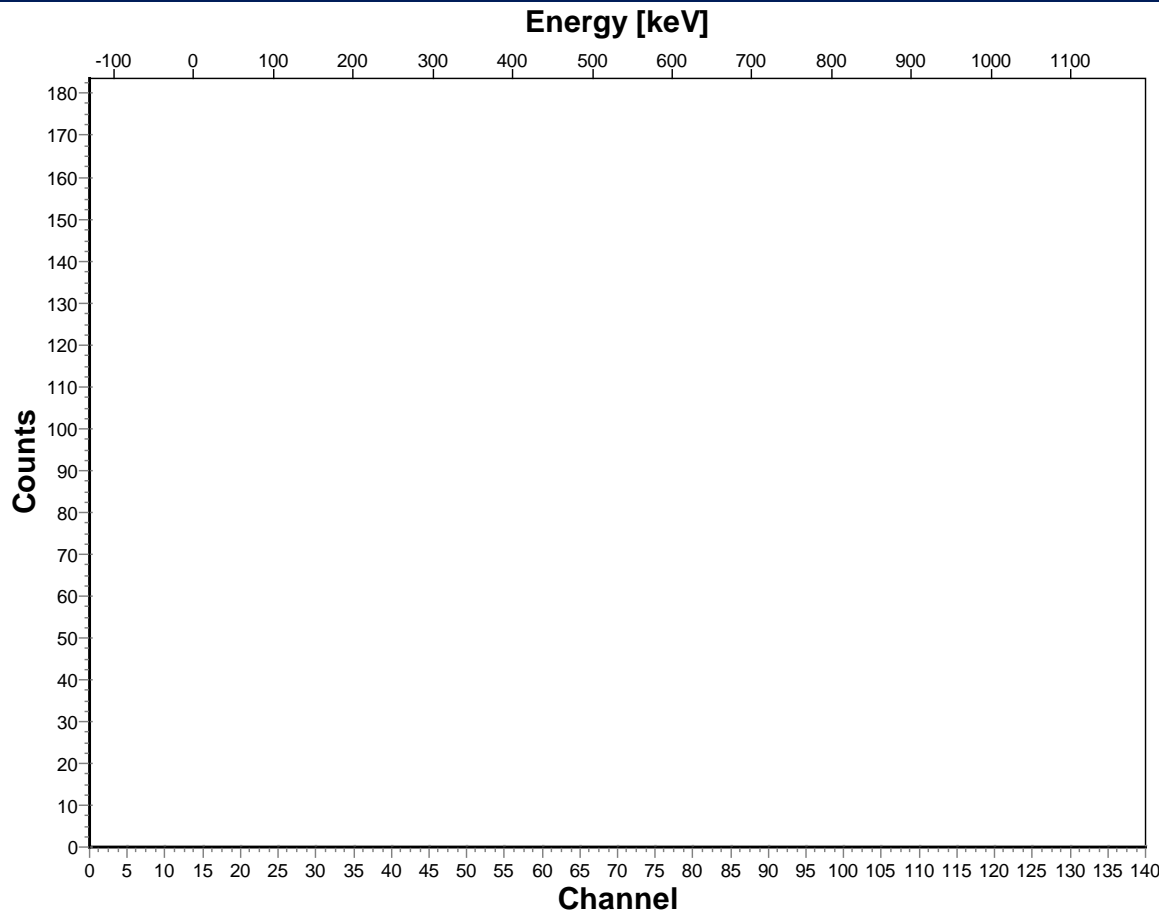
Hydrogen Concentration

Elastic Recoil Detection Analysis (ERDA) @ 4.3 MeV Li-7 beam



Elastically scattered
protons

Kapton ERDA

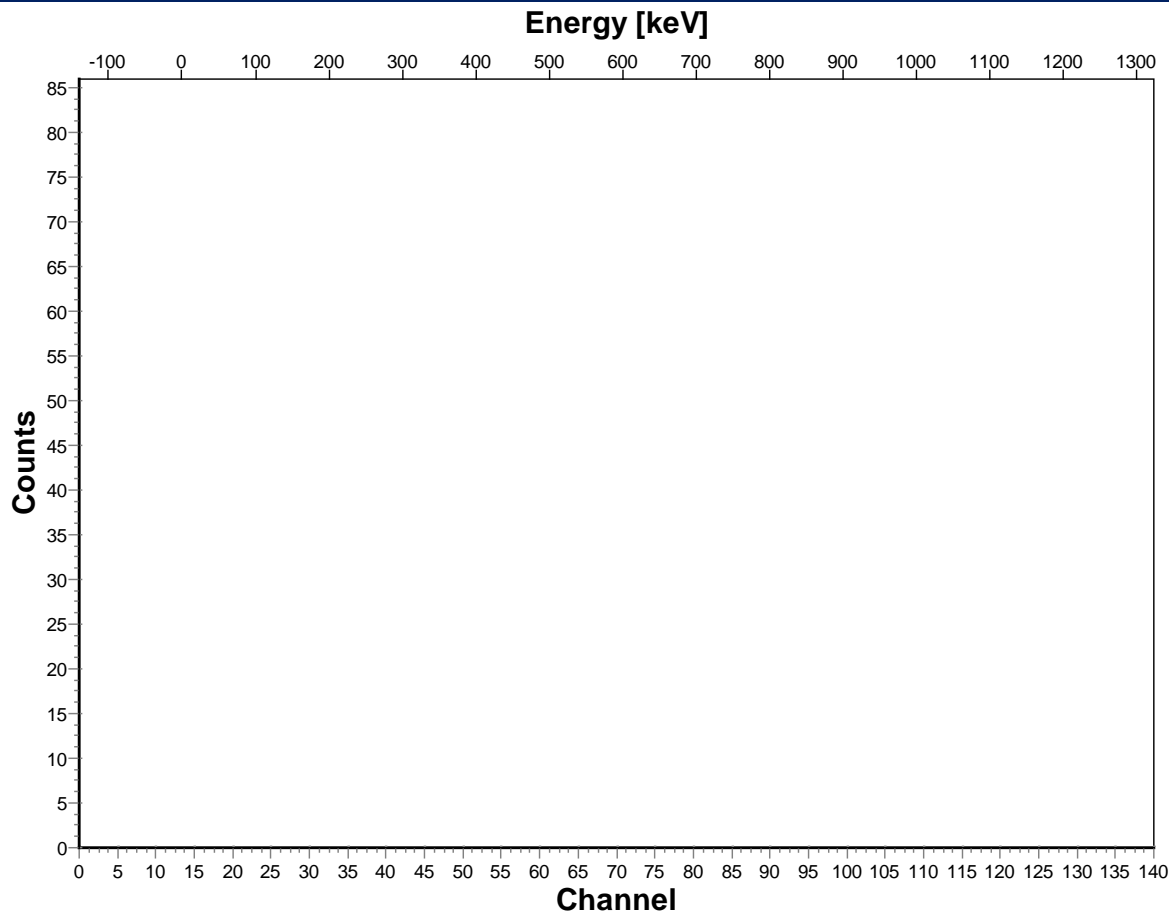


Proton spectrum
@ Li beam energy
of 4.3 MeV

Kapton ($C_{22}H_{10}N_2O_5$)
used for calibration

Simulated using SIMNRA, M. Mayer, Nucl. Instr. Meth. Phys. Res., **B194**, 177 (2002)
Cross sections from Z. Siketic et al., Nucl. Instr. Meth. Phys. Res., **B229**, 180 (2005)

Pd₇₅Ag₂₅ ERDA

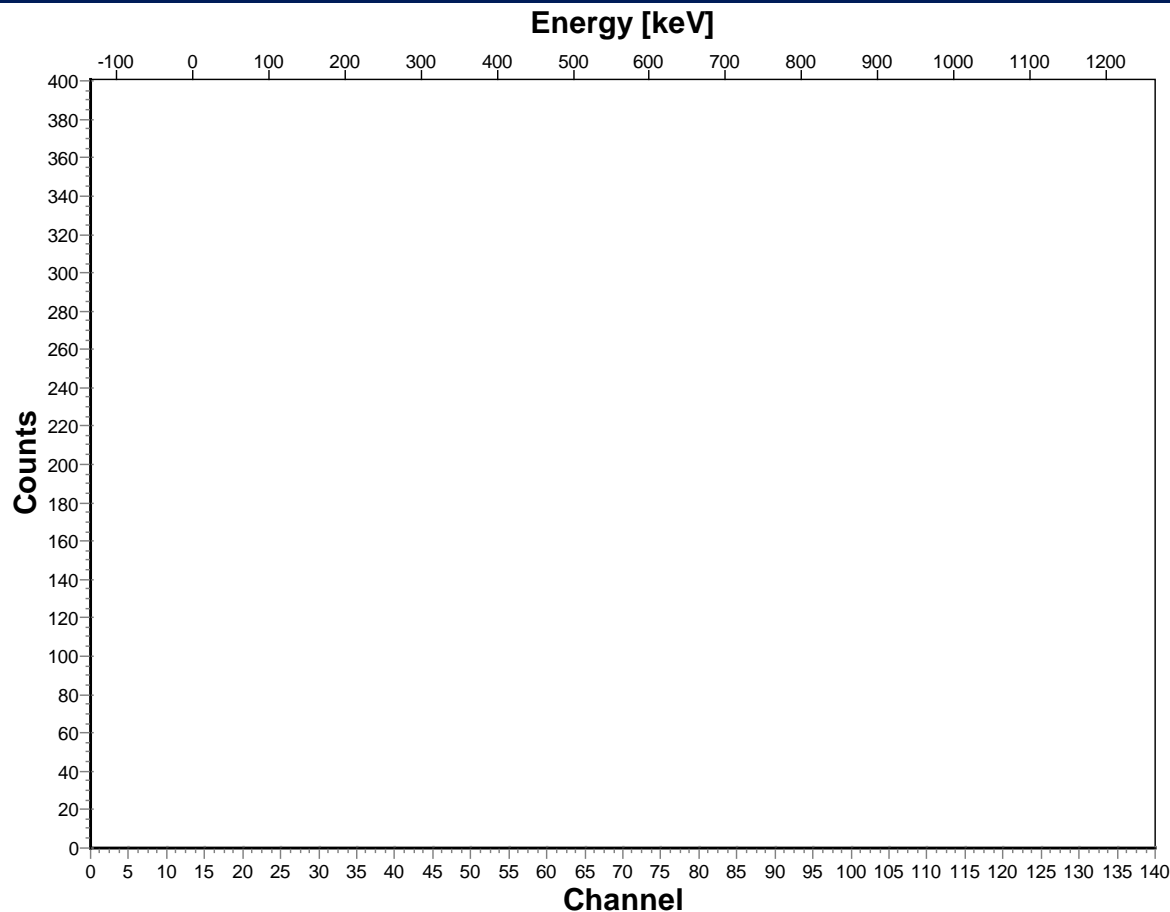


Proton spectrum
@ Li beam energy
of 4.3 MeV

SIMNRA gives
H/Pd ratio of 0.45%
and $4 \cdot 10^{16} \text{ cm}^{-2}$
H atoms on the
surface

Surface peak due to hydrogen dynamics

Pd ERDA



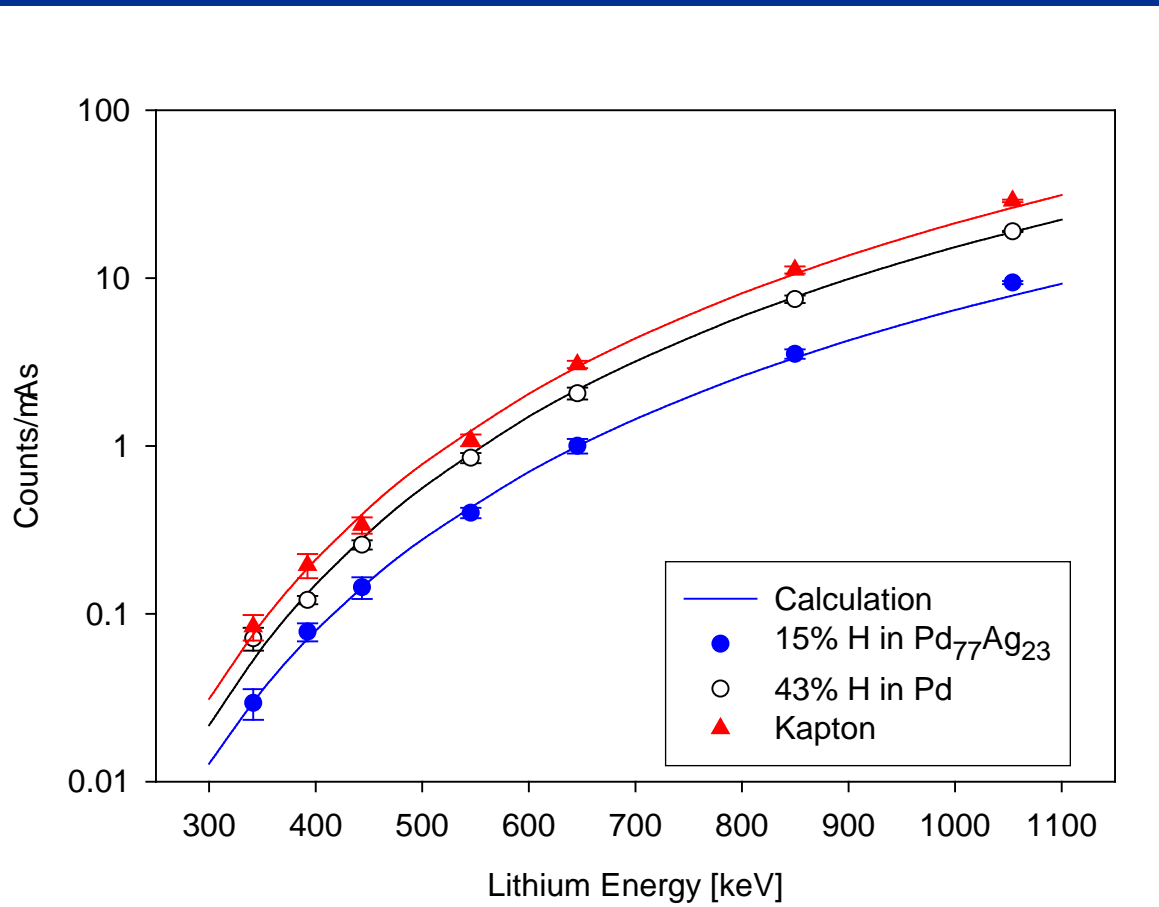
Proton spectrum
@ Li beam energy
of 4.3 MeV

SIMNRA gives
H/Pd ratio of 43 at.%
and a constant
depth profile

After heating at 900°C for 15 minutes in vacuum and
soaking in H₂ at 1 bar for 2 hours at room temperature

Thick Target Yields

$$\alpha\text{-particle yield calculation: } N_a = 2N_{Li} \frac{r N_A}{M} \int_{E_0}^0 \Omega W \frac{s(E)}{dE_{Li}/dx} dE_{Li}$$



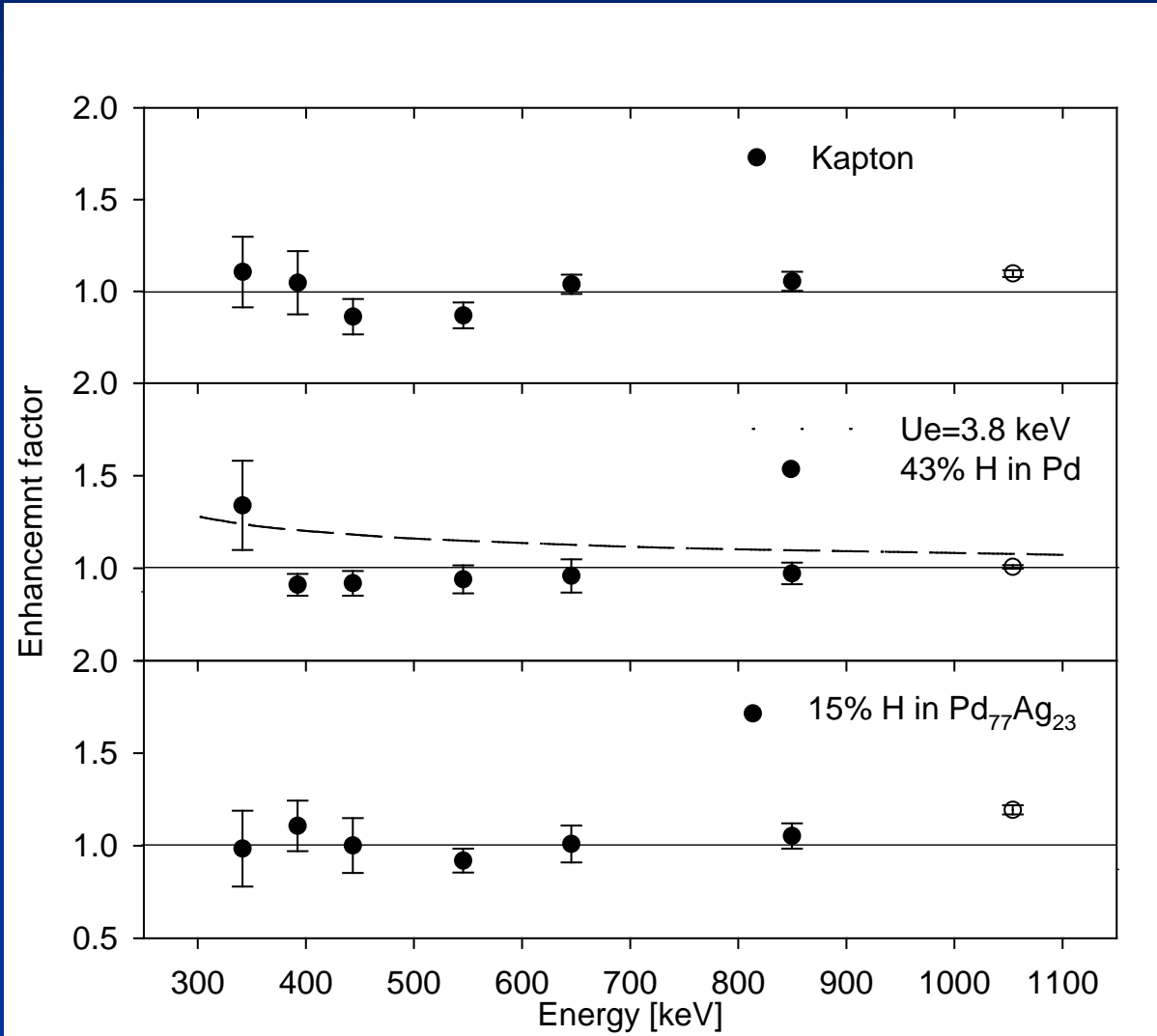
dE_{Li}/dx stopping power
 Ω efficiency
 W ang. distribution

Reaction: ${}^1\text{H}({}^7\text{Li}, \alpha){}^4\text{He}$

Enhancement Factors

$$f = N_{\alpha}(\text{measured}) / N_{\alpha}(U_e = 0)$$

Screening: $\sigma(E) \rightarrow \sigma(E + U_e)$

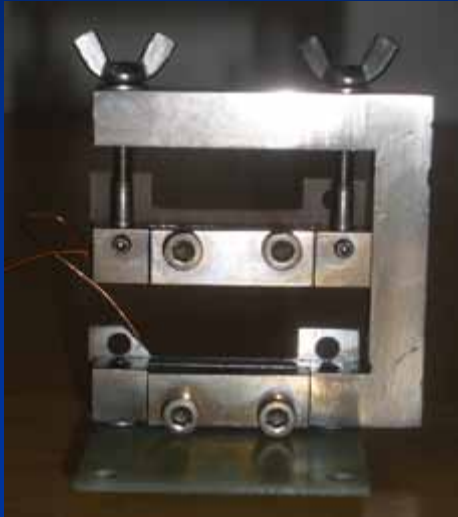


Kapton:
 $U_e < 0.6 \text{ keV}$

Pd:
 $U_e < 0.4 \text{ keV}$

Pd₇₇Ag₂₃:
 $U_e < 0.7 \text{ keV}$

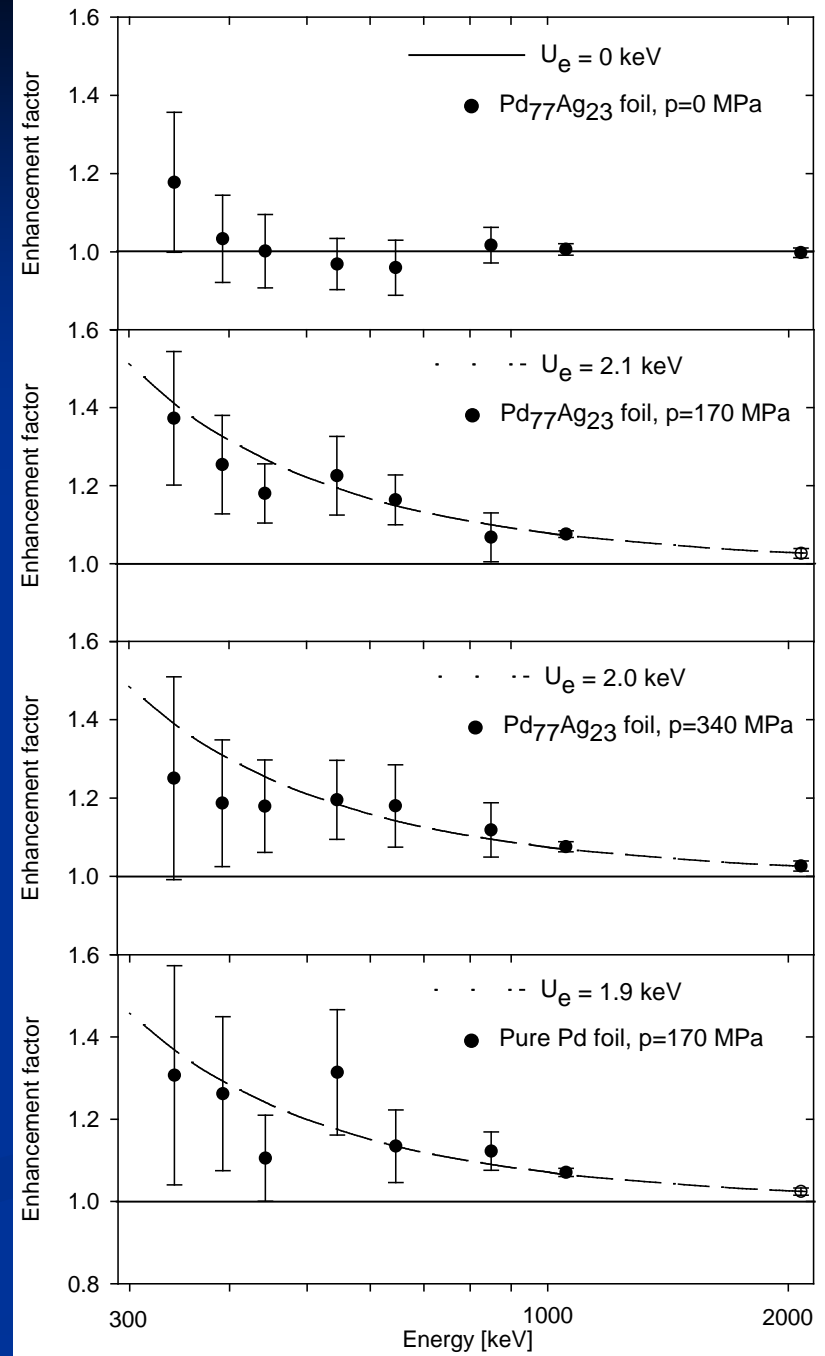
Results with stretching



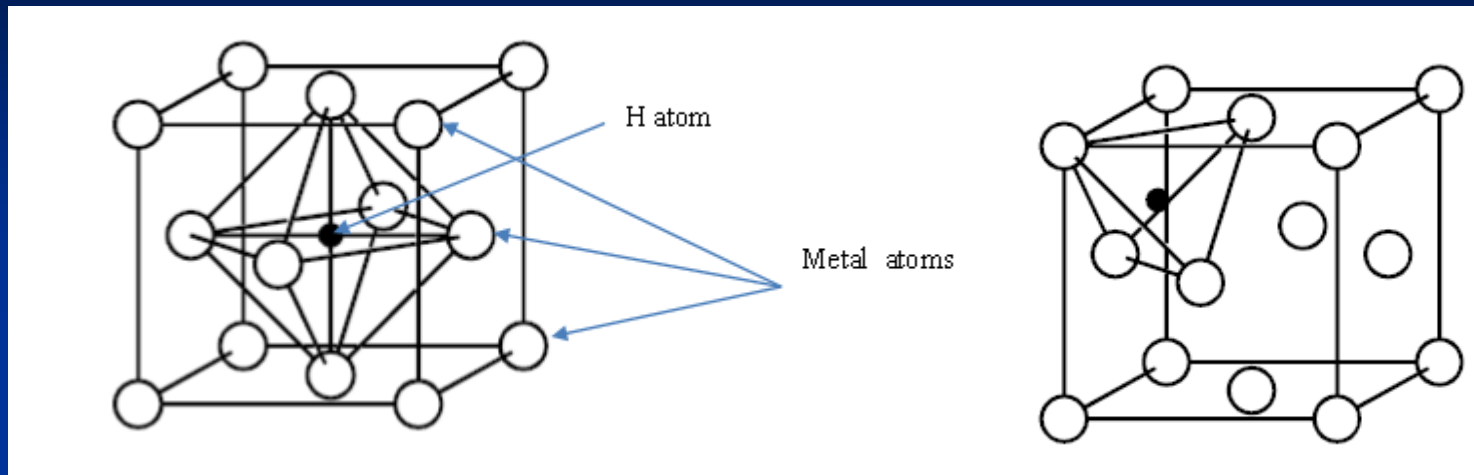
Targets, thicknesses, pressures and screening potentials

| Target | $d[\mu\text{m}]$ | H/M | $p[\text{MPa}]$ | $U_e[\text{keV}]$ |
|--------------------------------|------------------|----------|-----------------|-------------------|
| $\text{Pd}_{77}\text{Ag}_{23}$ | 125 | 0.562(5) | 340 | 2.0 ± 0.3 |
| $\text{Pd}_{77}\text{Ag}_{23}$ | 250 | 0.559(5) | 170 | 2.1 ± 0.2 |
| $\text{Pd}_{77}\text{Ag}_{23}$ | 250 | 0.599(5) | 0 | < 0.4 |
| Pd | 250 | 0.532(5) | 170 | 1.9 ± 0.2 |

M. Lipoglavsek et al., Eur. Phys. J. A44, 71 (2010).



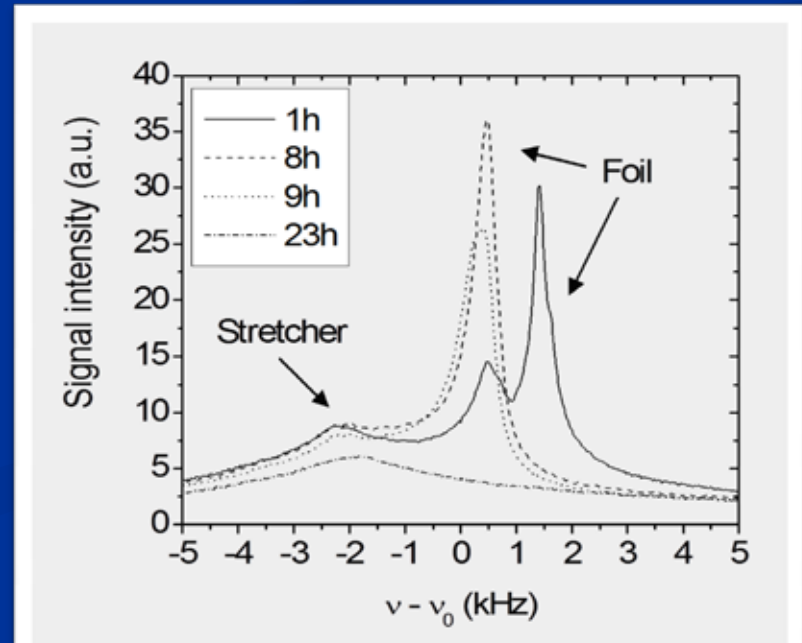
Possible explanation



face
centered
cubic
lattice

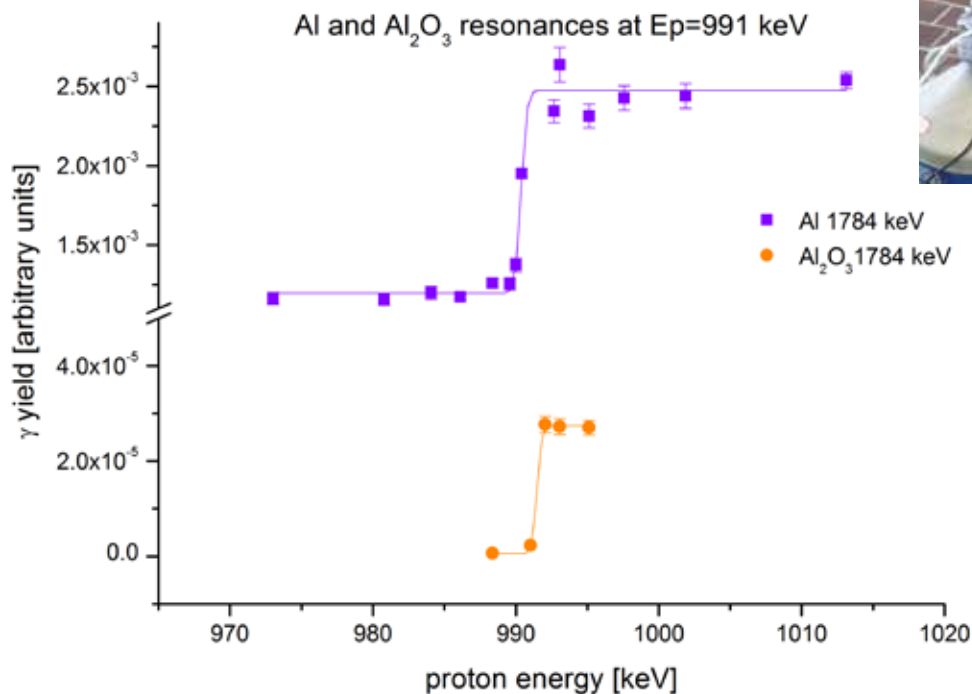
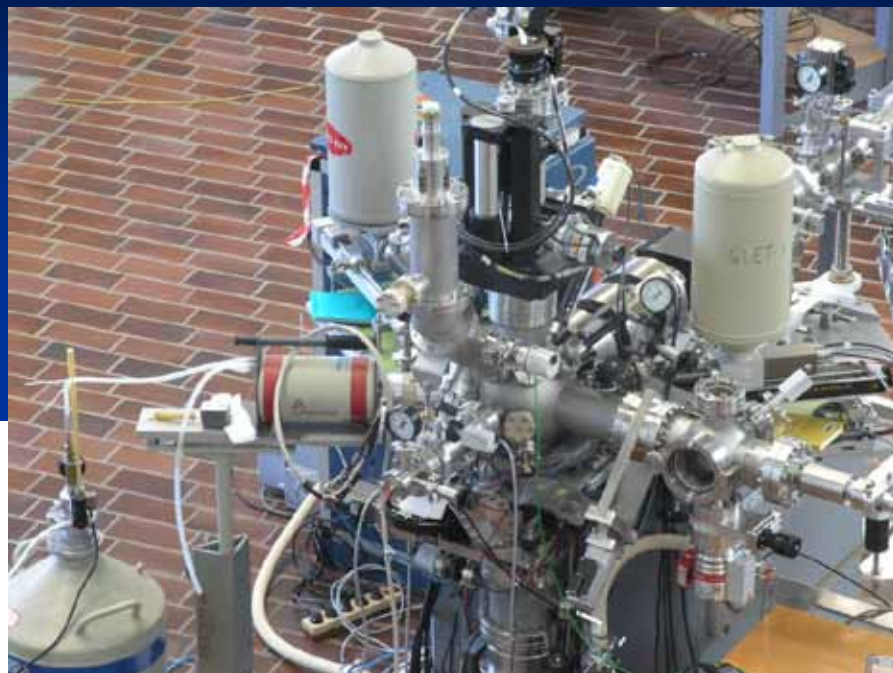
Octahedral position $\xrightarrow{\text{stretching}}$ Tetrahedral position

^1H NMR lineshapes measured by Hahn echo at $\nu_0 = 100$ MHz of a $250 \mu\text{m}$ thick Pd foil.



Electron screening in aluminum

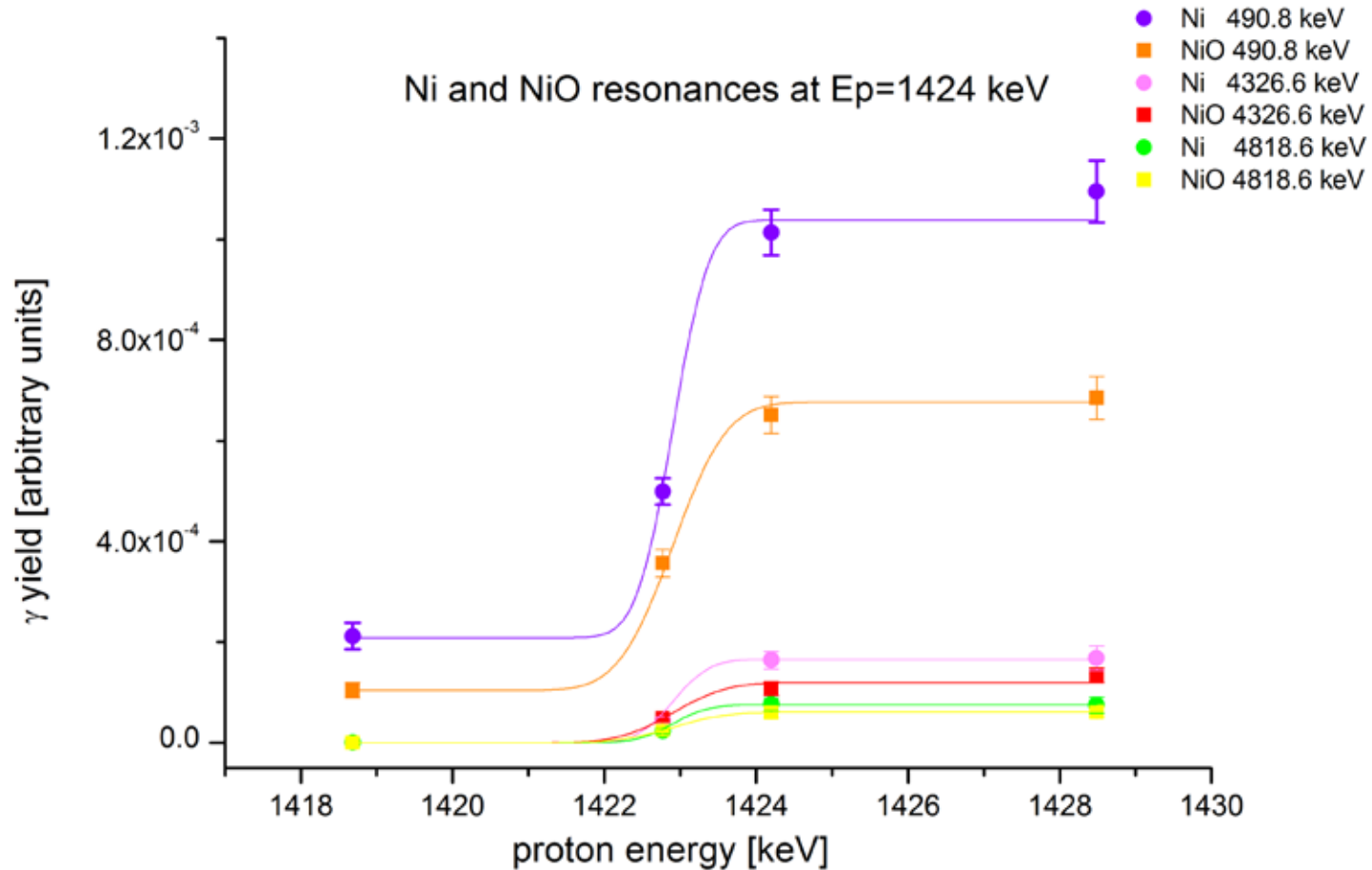
(p,γ) , $(p,p'\gamma)$ and $(p,n\gamma)$ reactions were studied on natural Ni and Al in metals, Pd₉₀Ni₁₀ alloy and NiO and Al₂O₃ insulators.



Characteristic γ rays were measured by a Ge detector: 1784 keV γ ray from $^{27}\text{Al}(p,\gamma)^{28}\text{Si}$ reaction

Nickel

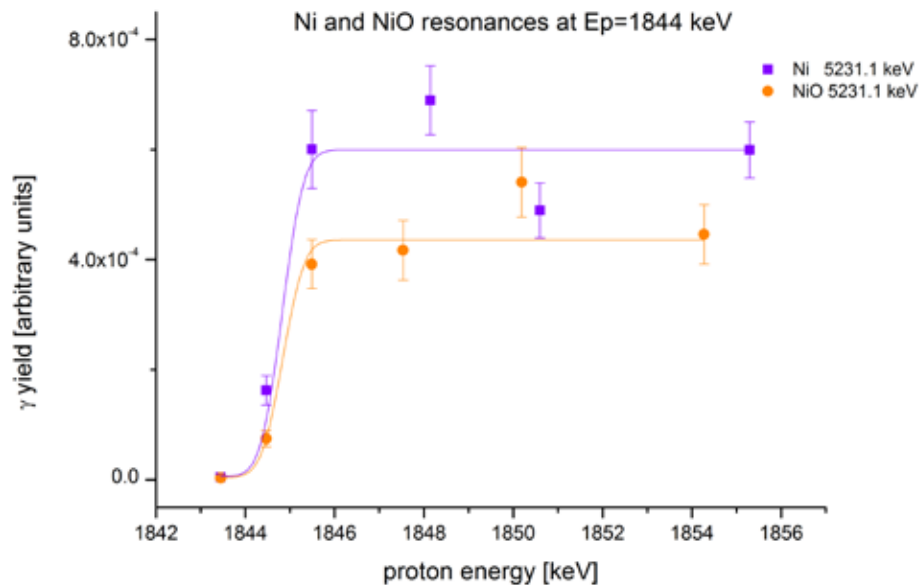
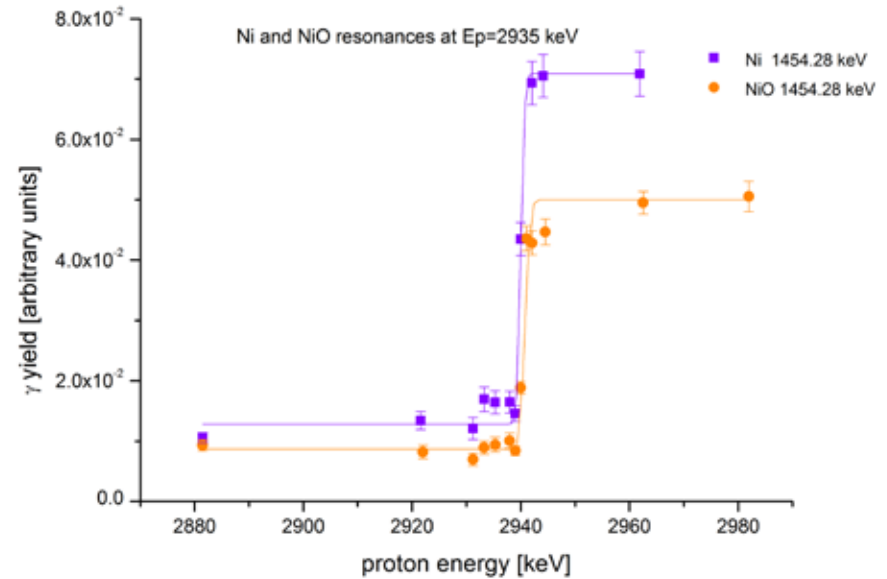
3 γ rays from $^{58}\text{Ni}(p,\gamma)^{59}\text{Cu}$ reaction



Nickel

1454 keV γ ray from $^{58}\text{Ni}(p,p'\gamma)^{58}\text{Ni}$ reaction

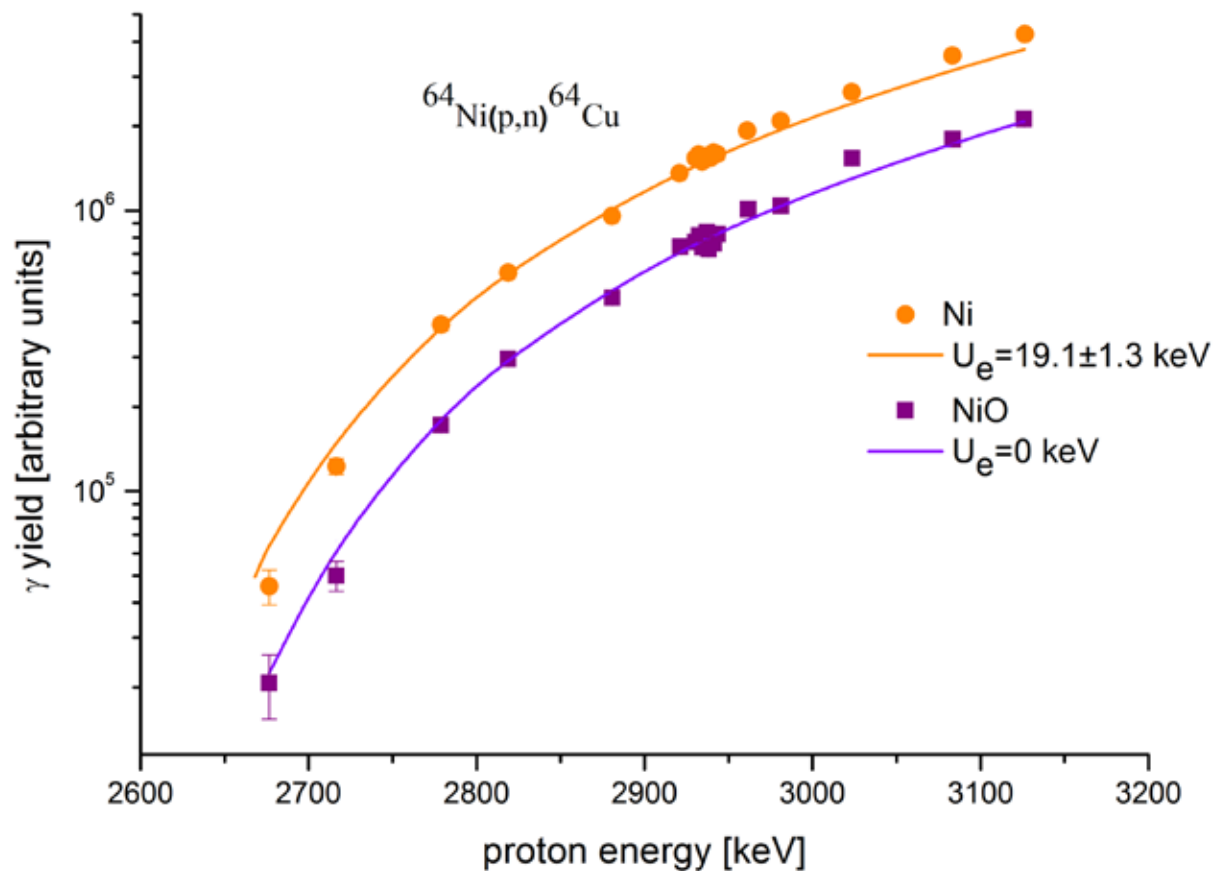
5231 keV γ ray from $^{58}\text{Ni}(p,\gamma)^{59}\text{Cu}$ reaction



- No shift in resonance energy
- No difference in resonance strength

$^{64}\text{Ni}(p,n)^{64}\text{Cu}$ reaction

$E_\gamma=159$ keV, very preliminary results



Conclusions

- n Electron screening in metals depends on H placement in the crystal
- n No large screening in slow compound nucleus reactions, (p,γ) and $(p,p'\gamma)$ resonances
- n At high Z only (p,n) reactions possibly show a large electron screening effect (to be confirmed) \rightarrow time scale of screening
- n Possible differences in β decay of copper isotopes